THE APPLICATION OF BAR CODING TECHNOLOGY AT WIPP

W. R. Chiquelin, Westinghouse WIPP Project
T. W. Halverson, Westinghouse WIPP Project
Carlsbad, NM 88220

ABSTRACT

Bar coding at the Waste Isolation Pilot Plant (WIPP) can be used to track waste containers within the facility, control transuranic (TRU) waste inventory flow, and reduce manpower and error in recording package identification or control parameters. By choosing where and when to bar code, precise timelines or time-and-motion studies can be conducted to aid in streamlining waste handling throughput at WIPP.

Additionally, the use of bar codes as waste container identification (ID) numbers increases the accuracy of recording the ID numbers by four orders of magnitude. The bar code label can also be utilized for other functions, such as shipping labels. Also, the bar code is integrated with the waste management data base such that the entire data base can be accessed on a computer using a bar code.

INTRODUCTION

Although not currently required in the Waste Isolation Pilot Plant (WIPP) waste acceptance criteria[1] and certification compliance documents for contact-handled waste[2,3], bar coding of waste package and six-pack identification numbers offers numerous advantages for material handling and inventory control. These advantages include:

1. Great increases in accuracy of data entry, speed of data entry, and labor savings achieved by minimizing manual data entry into the computer system;

2. Decreases in lag time between data acquisition and its availability for query and report writing; and

3. Decreases in the radiation dose to personnel who would otherwise spend a longer time near the waste packages to manually record the non-bar-coded waste package and six-pack identification numbers.

Bar Code Background

A bar code is a totally self-contained message encoded in the widths of bars and spaces in a printed pattern. The dark bars and light spaces represent ones and zeros, a binary language that computers utilize. Bar codes are read using an optical scanner, which sweeps a light beam across the bar code.

There are three types of scanners: contact wand, non-contact fixed beam, and non-contact moving beam laser. Moving beam scanners operate at the rates of up to 1500 scans per second. This enables multiple scans to be made, thus enhancing the reliability of the reading.

The more information there is in a bar code, the longer the bar code. The optical scanner feeds a bar code reader, which decodes the wave form signal into character inputs for a computer. Personal computers are adequate for bar coding.

Many bar code formats, known as bar code symbology, are currently used in the United States. The most familiar is the Universal Product Code (UPC) seen on food products and general merchandise. Each format has different characteristics such as length, numeric or alphanumeric capability, self-checking ability, and a different number of data characters in a set. Applications of the various codes range from retail stores, warehousing, and Department of Defense inventory control, to industrial and medical uses.

Bar Code Interface Working Group

Realizing the potential benefits, low cost, and simple nature of bar coding, the WIPP Project Office and the Transuranic (TRU) Waste Program Office of the U.S. Department of Energy in 1985 formed an Interface Working Group (IWG) to address bar coding of TRU waste containers. The IWG included members from WIPP and other TRU waste generator sites whose purpose was to assess the status of site bar coding activity, evaluate the costs and benefits of a standardized bar coding system for transuranic wastes, and provide a recommendation on coordinating bar coding activities with system-wide issues.

This IWG proposed that a standardized bar coding system, utilizing the Code 39 symbology, be implemented prior to shipments of contact-handled waste to the WIPP. Code 39 is a fully alphanumeric, self-checking, bidirectional, variable-length bar code, which is already used by the Department of Defense and can be printed by a wide variety of printing devices. Two bar code labels will be required on each drum, box, and six-pack of drums shipped to WIPP. These labels must have a minimum life of 20 years, be of medium density (5.4 characters per inch), and be black on white. The package identification number (PIN) in alphanumeric characters must be on each bar code label. The option is left open for sites to print package weight or other textual information on the label (such as shipping information or dose rate) at shipper discretion. This proposal allows each site the choice of equipment in implementing bar coding and the option to print bar code labels in-house or obtain them preprinted. In-house printing is advantageous since labeling costs are reduced by combining both a bar code and printed information on a printed label instead of stenciling or painting labels on waste containers.

The current WIPP plan includes the use of portable hand-held laser scanners along with both

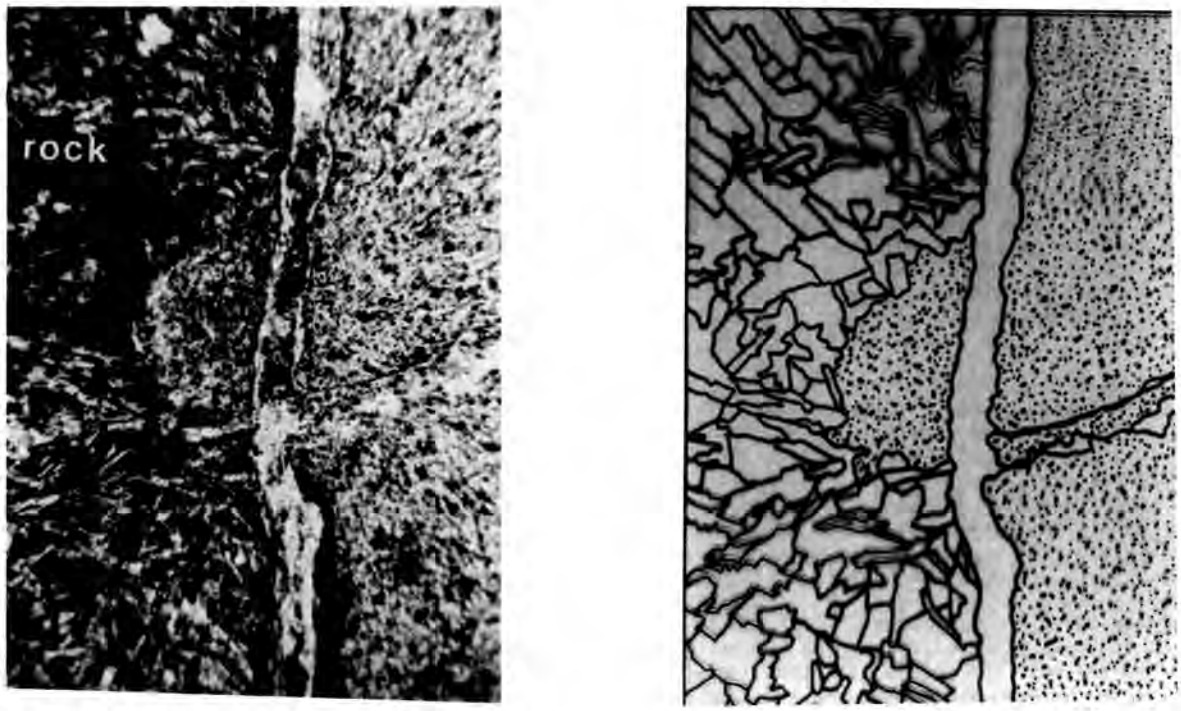

(a) (b)

Fig. 1. Photomicrograph (a) of the rock-cement interface (sample MICRO-A). The picture covers an area of 2.5 mm x 4.0 mm. The interface aperture (0.2 mm) probably is produced by the shrinkage of the cement plug during preparation of the thin section. System 1 cement is poured in a 38 mm diamond drilled hole of Grande basaltic andesite. The drawing (b) shows a clear outline of the micrograph.

representative features of the borehole plug. Four specimens are cut along the hole length. Each specimen has an approximate size of 3 x 2 x 0.5 cm.

(d) In order to dry the specimen, two specimens (sample nos. MICRO-A and MICRO-B) are placed on a heat pan generating a temperature of 260°C for 1 hour. Other specimens (sample nos. MICRO-C and MICRO-D) are dried at 45°C for 7 days.

(e) The dried specimen is attached to a piece of glass and ground to a thickness of 50 microns.

(f) Dye is applied to the thin section to enhance the discontinuities (cracks, flow layers, etc.). A cover glass is used to prevent the dye from fading away.

Microscopic Results

For samples MICRO-A and MICRO-B [dried at high temperature (260°C)], the width of the rock-cement interface is measured as 0.2 mm and seems to be constant along the borehole length (Fig. 1 and 2). The width of the shrinkage cracks within the cement itself varies from 0.001 mm to 0.1 mm. These cracks appear throughout the plug with an intensity of 1 per 2 mm. The cement particle sizes approximated by microscopic observation at a magnification of 40 diameters vary from 1×10^{-4} mm to 700×10^{-4} mm. The size distribution is poorly graded; fifty percent of the particles range from 1×10^{-4} to 10×10^{-4} mm, and the rest have sizes ranging from 0.01 to 0.07 mm. Figure 3 shows the cement particles penetrating into the rock flow layers near the borehole wall, presumably before the cement solidifies. For both samples, observation along the borehole length indicates that cement particles penetrate along fifty percent of the intergranular cracks induced by drilling, even though the cement plugs in these experiments are simply poured, i.e. not pressurized during or after pouring. Ten percent of the interface is occupied by air bubbles (Fig. 3). The rest of the hole length shows no indication of the cement penetration. The cement porosity can not be determined due to insufficient magnification of the microscope.

For samples MICRO-C and MICRO-D [dried at less elevated temperatures (45°C)], the width of the rock-cement interface is measured as 0.1 mm and tends to be constant along the borehole length. The cement plug itself shows some shrinkage cracks with an average width of 0.01 mm. The crack intensity is approximately 1 per centimeter. Fifty percent of the microcracks in the borehole wall along the borehole length are penetrated by cement particles. The smallest cracks filled by the cement particles are found to be 50 microns wide (Fig. 4). The cement particles might penetrate into some smaller cracks; however, due to the limit of the microscope, those cracks can not be identified unambiguously. All rock flow layers near the borehole wall, usually found as 0.5-1.0 mm wide, are partially filled with cement particles (Fig. 5). The size distribution of the cement particles observed from these two samples is similar to the one observed from the samples MICRO-A and MICRO-B.

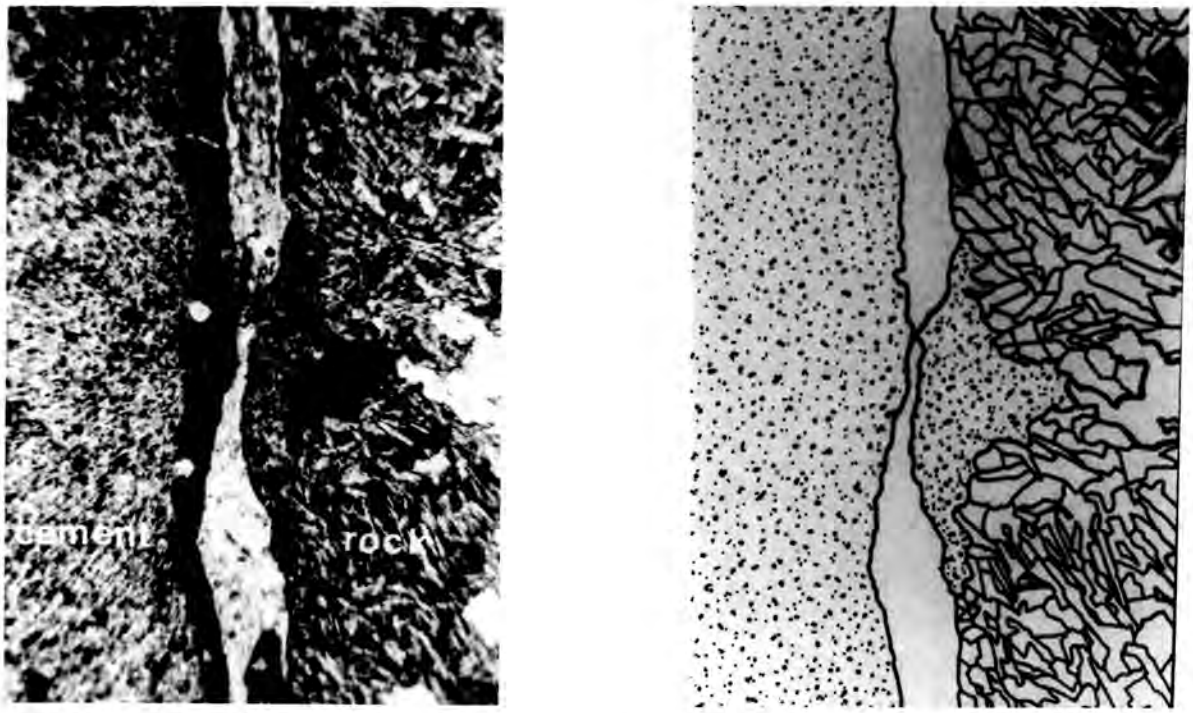

(a) (b)

Fig. 2. Photomicrograph (a) of the rock-cement interface (sample MICRO-B). The picture covers an area of 2.5 mm x 4.0 mm. The interface aperture (0.2 mm) probably results from shrinkage of the cement plug during preparation of the thin section. System 1 cement is poured in a 38 mm diamond drilled hole of Grande basaltic andesite. The drawing (b) shows a clear outline of the micrograph.

Discussion of the Microscopic Results

Comparison of the results obtained from the low temperature drying samples with the results obtained from the high temperature drying samples indicates that the drying temperature affects the shrinkage characteristics of the cement plug. Higher drying temperatures induce more shrinking, as indicated by wider interface aperture, wider cement shrinkage cracks, and higher crack intensity within the cement.

Adisoma and Daemen[5] backcalculate the width of the borehole interface between System 1 cement and Charcoal granite from the flow rate through a dried-out plug as 1×10^{-3} mm. The interface width measured as 0.1 mm (for low temperature drying samples) is significantly wider than the calculated one. The difference might be caused by a combination of the following factors:

(a) Grinding. The microscopic specimens have to be ground to a 50 micron thickness. The grinding powder might widen the interface (which initially might be small).

(b) Adisoma and Daemen[5] allow the cement plug to dry in a 25 mm hole in a granite sample. Even though the period of drying-out for the sample is up to 9 months, the cement plug in the hole might not be completely dehydrated. The water trapped in some isolated voids within the cement may cause some expansion.

(c) The drying-out of the cement plug in granite as performed by Adisoma and Daemen[5] might leave some cement fragments (resulting from cement shrinkage cracks) along the interface. These fragments might become obstacles to water flow along the interface.

According to the factors described above, the microscopic results might overestimate the interface width as compared to the actual sealing conditions. The results of simulating the condition of drying-out cement plugs are, therefore, more reliable. Microscopic observations do provide a direct visual

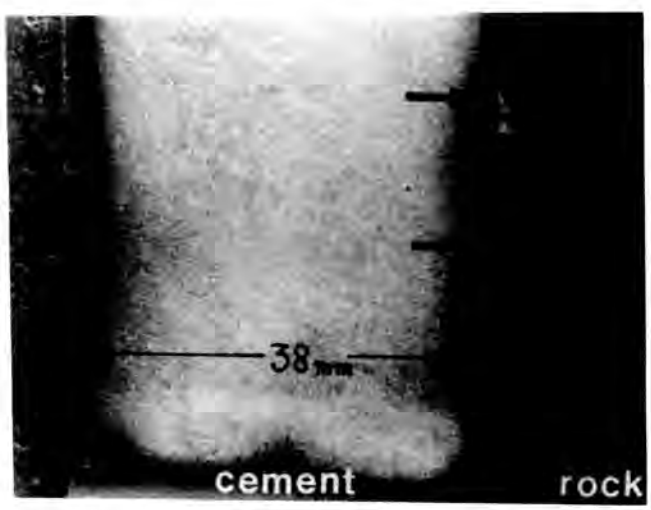

Fig. 3. Cross-section of half of a 38 mm cement plug in a diamond drilled hole of Grande Basaltic andesite. The picture covers an area of 64 mm x 40 mm. The circles indicate cement particles that have penetrated into the rock flow layers. The arrows indicate air bubbles trapped along the interface.

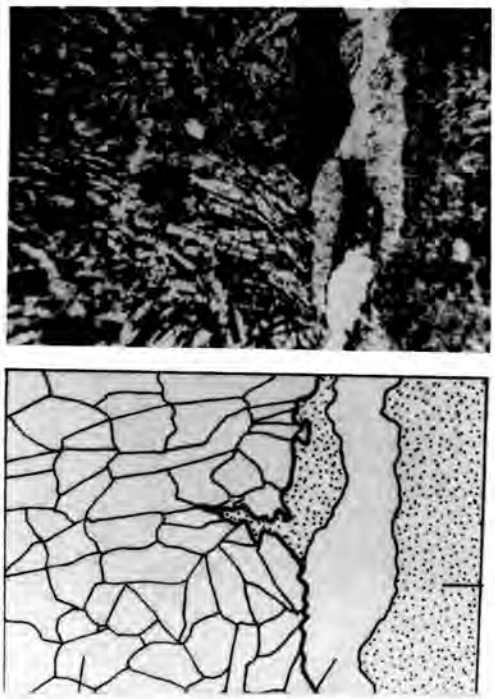

Fig. 4. Photomicrograph (top) shows cement particles that penetrated into a microcrack (sample MICRO-C). The width of the crack is 50 microns. The micrograph covers an area of 1.00 x 2.00 mm. The interface aperture (0.1 mm) results from shrinkage of the cement plug. The drawing (bottom) shows a schematic outline of the micrograph.

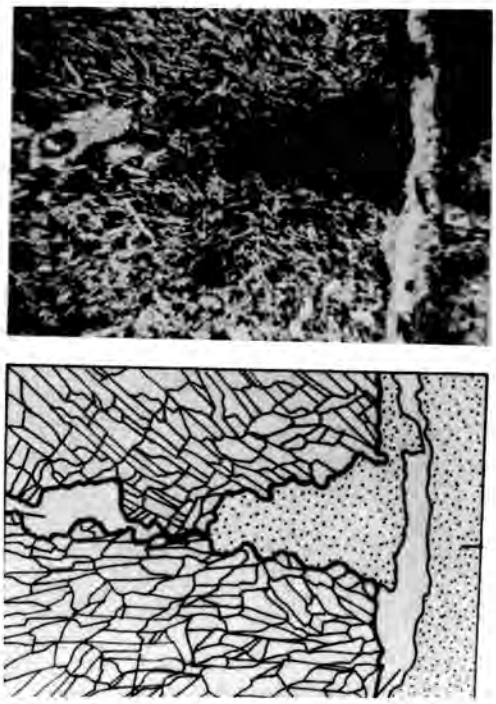

Fig. 5. Photomicrograph (top) shows cement particles that have penetrated into a basalt flow layer (sample MICRO-D). The width of the layer is approximately 0.5 mm. The micrograph covers an area of 2.50 x 4.00 mm. The drawing (bottom) shows a schematic outline of the micrograph.

estimate of what probably is an upper bound on the interface shrinkage separation.

Schaffer and Daemen[18] determine the effectiveness of using Portland cement grouts as sealants of fractures normal to 25 mm boreholes in Charcoal granite. Using an injection pressure of 5.5 MPa, the smallest fracture aperture penetrated by cement grout is found to be 92 microns. In this investigation, even though the borehole cement plug has not been pressurized during or after pouring, the smallest crack penetrated by cement particles is found to be only 50 microns wide. Considering the high probability that rock grouting at seal locations will be required, especially in hard jointed rock, in order to prevent bypass flow around the seals, it appears that further investigation is warranted in order to try to explain this discrepancy.

CEMENT SWELLING PRESSURE

The swelling pressure of a cement plug is of interest since it might be one of the factors controlling the permeability of the rock-cement interface. The swelling pressure (or expansive stress) studied here is the pressure created by the radial expansion of the cement plug cured over a period of time. The cement expansive stress is, also, one of the significant factors governing the axial strength of cement borehole plugs (i.e. strength of a plug increases as cement expansive stress increases[19]).

Swelling tests have been performed to determine some expansion characteristics of swelling cement cylinders by pouring and curing the cement under atmospheric pressure in 64 mm I.D. steel cylinders and measuring the tangential strains of the cylinder outer surface by means of electrical strain gages. Using different cylinder thicknesses (1.8, 3.1 and 4.2 mm), the expansive stresses are obtained for different radial strains. The expansive stresses and radial strains are calculated using equations derived from Jaeger and Cook:[20]

$$\sigma_r = \frac{E\varepsilon_t}{2R_1^2/(R_2^2 - R_1^2)(1 - \nu^2)} \tag{1}$$

$$u = \frac{\sigma_r R_1^3}{2(\lambda + G)(R_2^2 - R_1^2)} \quad \frac{\sigma_r R_1 R_2^2}{2G(R_2^2 - R_1^2)} \tag{2}$$

$$\varepsilon_r = u/R_1 \tag{3}$$

where σ_r = expansive stress in Mpa
E = Young's modulus of steel pipe = 207×10^3 MPa
ε_t = measured tangential strain
ν = Poisson's ratio of steel pipe = 0.27
R_1 = inside radius of pipe in meters
R_2 = outside radius of pipe in meters
u = radial displacement in meters

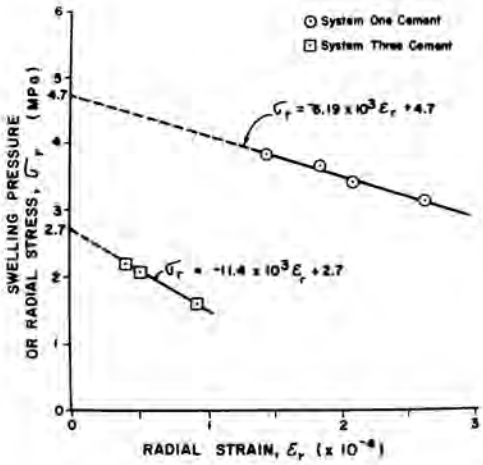

Fig. 6. Swelling pressures of cement mixes as a function of radial strain. The pressures have been measured after cement curing for 25 days. The cement diameter is 64 mm. Extrapolation of the linear equation to the condition of no strain allowed indicates a maximum swelling pressure of up to 4.7 MPa for System 1 cement, and up to 2.7 MPa for System 3 cement.

λ = Lame's parameter = 9.567×10^4 MPa for steel pipe
G = Lame's parameter = 8.149×10^4 MPa for steel pipe
ε_r = radial strain of cement cylinder.

The calculated expansive stresses for System 1 and System 3 cements cured for 25 days are plotted as a function of radial strain in Fig. 6. A linear equation is proposed to describe the relation between the swelling pressure and the radial strain:

$$\sigma_r = m_e(\varepsilon_r) + SP_{(max)} \qquad (4)$$

where σ_r = radial stress in MPa,
m_e = expansion modulus in MPa, and
$SP_{(max)}$ = maximum swelling pressure in MPa.

Using least square fitting, the expansion moduli for System 1 and System 3 cements are calculated as -6.19×10^3 MPa and -11.4×10^3 MPa, respectively. The maximum swelling pressures obtained by extrapolation of the curve to the condition of no strain allowed ($\varepsilon_r = 0$) are approximately 4.7 MPa for System 1 cement and 2.7 MPa for System 3 cement (Fig. 6). It deserves pointing out that both the maximum swelling pressure and expansion modulus depend on the size (cylinder diameter), the type of cement and grout mix, the curing time, and curing conditions.

At the same curing period (here 25 days), the System 1 cement shows better performance (higher maximum swelling pressure and higher volumetric expansion) than does the System 3 cement. In actual borehole or shaft sealing, the swelling pressure of a cement plug may not reach the maximum if the rock around the borehole has a low stiffness (low Young's modulus, E), i.e. lower stiffness rock allows larger radial strain of a plug and leads to the lower cement expansive stress. Also, this may cause a decrease of the axial strength of the borehole plug.

Fuenkajorn and Daemen[10,11] show that drilling induces a damage zone around boreholes. The zone consists mainly of cleavage fractures and intergranular cracks, and is not likely to extend more than 7 percent of the borehole radius into the borehole wall, irrespective of drilling method. The permeability of the damaged zone has an insignificant effect on the borehole plug performance. These conclusions agree with the conclusions drawn by Lingle et al.[21] and Burns et al.[7] The low permeability of the damaged zone might be due to (1) the small aperture and length of the cracks, (2) lack of connectivity between the cracks, (3) closure of the cracks due to swelling pressure of cement plug, (4) infiltration of cement particles into the cracks, or (5) secondary mineralization within the cracks. Even though the damage zone has low permeability, it may appear as a weak zone (i.e. has lower stiffness than the undamaged rock) surrounding the borehole plug. This weak zone may allow a larger radial strain for a borehole cement plug which could lead to a low swelling pressure obtained at the cement plug-rock interface.

The swelling pressures observed (e.g. nearly 5 MPa) clearly are of a sufficient magnitude to raise concern about what the effect of excessive swelling pressures might be on the rock barrier directly adjacent to any seals. Related laboratory experiments[22,23] have resulted in tensile fractures under some (admittedly unfavorable) conditions. It can readily be visualized that the tangential tensile stress induced by seal swelling could have the effect of increasing the aperture of unfavorably oriented rock fractures, particularly so around underground excavations in a rock mass subjected to highly anisotropic stressfields. For this reason it would seem that considerable more work on determining swelling pressures, and the factors that influence their development, is needed.

CONCLUSIONS

The widths of the rock-cement plug interface are measured by microscopic observation as 0.1 mm for sample dried at 45°C and as 0.2 mm for samples dried at 260°C. Higher drying temperatures induce not only wider interface aperture, but wider cement shrinkage cracks and higher crack density within the cement. Fifty percent of the microcracks and all rock flow layers in the borehole wall are penetrated by cement particles. The smallest cracks penetrated by cement particles are found to be 50 microns wide. The swelling pressure (radial expansive stress) of 64 mm cement plugs (System 1 and 3) tends to decrease linearly as increasing radial strain is allowed. Therefore, one of the factors governing the expansion characteristics of a borehole cement plug is the stiffness of the surrounding rock.

ACKNOWLEDGMENT

This work is a part of an ongoing research effort on rock mass sealing, Contract NRC-04-78-271, supported by the Division of Radiation Programs and Earth Sciences, Office of Nuclear Regulatory Research, U.S. Nuclear Regulatory Commission.

REFERENCES

1. C. M. KOPLICK, D. L. PENTZ, and R. TALBOT, "Borehole and Shaft Sealing - Information Base for

Waste Repository Design," Vol. 1, NUREG/CR-0495, NTIS: PB 293401, prepared for the U.S. Nuclear Regulatory Commission by the Analytic Sciences Corporation, Reading, Massachusetts (1979).

2. P. KELSALL, "Penetration Characteristics of Seal Design," Presentation 3, pp. 22-23, D'Appolonia Consulting Engineers, Proc. Repository Sealing Field Testing Workshop, ONWI-239, prepared for the Office of Nuclear Waste Isolation, Battelle Memorial Institute, Columbus, Ohio (1980).

3. I. W. MARINE, "Review Comments," Section 6, pp. 15-17, in D'Appolonia Consulting Engineers, Proc. Repository Sealing Field Testing Workshop, ONWI-239, prepared for the Office of Nuclear Waste Isolation, Battelle Memorial Institute, Columbus, Ohio (1980).

4. M. J. SMITH and S. C. McCAREL, "Basalt Waste Isolation Project Borehole Plugging Studies - An Overview," pp. 131-141, Proc. Borehole and Shaft Plugging, workshop jointly organized by the OECD Nuclear Energy Agency and the U.S. Dept. of Energy, Columbus, Ohio, May. Published by OECD NEA, Paris, France (1980).

5. G. S. ADISOMA and J. J. K. DAEMEN, "Laboratory Assessment of the Effect of Drying on the Performance of Cement Borehole Plugs," Waste Management '84 Symposium, Tucson, AZ, March 11-15, Vol. 1, pp. 579-583 (1984).

6. D. L. SOUTH and J. J. K. DAEMEN, "Permeameter Studies of Water Flow through Cement and Clay Borehole Seals in Granite, Basalt, and Tuff," Technical Report to the U.S. Nuclear Regulatory Commission, Division of Radiation Programs and Earth Sciences, Contract NRC-04-78-271, by the Department of Mining and Geological Engineering, University of Arizona, Tucson (1986).

7. F. L. BURNS, R. LINGLE, and A. ANDREWS, "Cement-Plug Leakage and Drilling Damage Evaluated," Oil and Gas Journal, Nov. 22, Vol. 80, no. 22, pp. 120-129 (1982).

8. J. J. K. DAEMEN, W. B. GREER, G. S. ADISOMA, K. FUENKAJORN, W. D. SAWYER, Jr., A. YAZDANDOOST, H. AKGUN, and B. KOUSARI, "Annual Report, Rock Mass Sealing, June 1, 1983 - May 31, 1984," NUREG/CR-4174, prepared for the U.S. Nuclear Regulatory Commission, Division of Health, Siting and Waste Management, by the Department of Mining and Geological Engineering, University of Arizona, Tucson (1985).

9. T. O. ALLEN and A. P. ROBERTS, "Production Operations," Oil and Gas Consultants International, Inc., Tulsa, Oklahoma (1982).

10. K. FUENKAJORN and J. J. K. DAEMEN, "Experimental Assessment of Borehole Drilling Damage in Basaltic Rocks, Proc. of 25th U.S. Symposium on Rock Mechanics Northwestern University, Evanston, Illinois, pp. 774-783 (1984).

11. K. FUENKAJORN and J. J. K. DAEMEN, "Borehole Drilling Damage in Basaltic Rocks," Technical Report to the U.S. Nuclear Regulatory Commission, Division of Radiation Programs and Earth Sciences, Contract NRC-04-78-271, by the Department of Mining and Geological Engineering, University of Arizona, Tucson (1986).

12. AMERICAN PETROLEUM INSTITUTE, "Specification RP-10B, Testing Oil, Cement and Cement Additives," Twentieth Edition, API, Dallas, Texas, April (1977).

13. M. E. HARR, Groundwater and Seepage, McGraw-Hill Book Co., Inc., New York (1962).

14. J. J. K. DAEMEN, D. L. SOUTH, W. B. GREER, J. C. STORMONT, S. A. DISCHLER, G. S. ADISOMA, K. FUENKAJORN, D. E. MILES, B. KOUSARI, and J. BERTUCA, "Annual Report, Rock Mass Sealing, June 1, 1982 - May 31, 1983," NUREG/CR-3473, prepared for the U.S. Nuclear Regulatory Commission, Division of Health, Siting and Waste Management, by the Department of Mining and Geological Engineering, University of Arizona, Tucson (1983).

15. D. M. ROY, M. W. GRUTZECK, and P.H. LISCASTRO, "Technical Report - Evaluation of Cement Borehole Plug Longevity," ONWI-30, prepared for Office of Nuclear Waste Isolation, by Material Research Laboratory, Pennsylvania State University, University Park, PA (1979).

16. G. SIMMONS and L. CARUSO, "Microcracks and Radioactive Waste Disposal," Scientific Basis for Nuclear Waste Management VI, Materials Research Society Symposia Proceedings, Vol. 15, pp. 331-336 (1983).

17. J. A. APPS, "Hydrothermal Evolution of Repository Groundwater in Basalt," NRC Nuclear Waste Geochemistry '83, Proceedings of the U.S. Nuclear Regulatory Commission, U.S. Geological Survey National Center, Reston, Virginia, pp. 14-51 (1984).

18. A. SCHAFFER and J. J. K. DAEMEN, "Permeability Testing and Grouting of Fractured Rock," Technical Report to the U.S. Nuclear Regulatory Commission, Division of Radiation Programs and Earth Sciences, Contract NRC-04-78-271, by the Department of Mining and Geological Engineering, University of Arizona, Tucson (1986).

19. J. C. STORMONT and J. J. K. DAEMEN, "Axial Strength of Cement Borehole Plugs in Granite and Basalt," NUREG/CR-3594, Topical Report on Rock Mass Sealing, prepared for the U.S. Nuclear Regulatory Commission, Division of Health, Siting and Waste Management, by the Department of Mining and Geological Engineering, University of Arizona, Tucson (1983).

20. J. C. JAEGER and N. G. W. COOK, Fundamentals of Rock Mechanics, 3rd edition, Chapman and Hall, London (1979).

21. R. LINGLE, K. L. STANFORD, P. E. PETERSON, and S. F. WOODHEAD, "Technical Report, Wellbore Damage Zone Experimental Determination," ONWI-349, prepared for Office of Nuclear Waste Isolation by Terra Tek, Inc., University Research Park, Salt Lake City, Utah (1982).

22. H. AKGUN and J. J. K. DAEMEN, "Size Effects on Borehole Plug Performance," Technical Report to the U.S. Nuclear Regulatory Commission, Division of Radiation Programs and Earth Sciences, Contract NRC-04-78-271, by the Department of Mining and Geological Engineering, University of Arizona, Tucson (1986).

23. J. J. K. DAEMEN, W. B. GREER, K. FUENKAJORN, H. AKGUN, T. S. AVERY, J. WILLIAMS, A. F. KIMBRELL, A. SCHAFFER, and B. KOUSARI, "Annual Report, Rock Mass Sealing, June 1, 1984 - May 31, 1985," prepared for the U.S. Nuclear Regulatory Commission, Division of Radiation Programs and Earth Sciences, Contract No. NRC-04-78-271, by the Department of Mining and Geological Engineering, University of Arizona, Tucson (1986).